Supplemental Information

I. Sequential rinsing studies of $(CH_2)_5COOH/(CH_2)_4OH$ covalent assemblies with no rate monitoring

SAMs composed of 2:3 $(CH_2)_5COOH/(CH_2)_4OH$ were prepared on gold ball electrodes via immersion in a 2:3 molar ratio solution of the corresponding thiols in ethanol. Electrostatic assemblies were prepared by 30-60 minute immersion in cytochrome *c* solution (30-40 μM in 4.4 mM pH=8 potassium phosphate buffer), while covalent assemblies were prepared by successive 30-60 minute immersion periods in *N*-cyclohexyl-*N′*-(2-morpholinoethyl)carbodiimide methyl-*p*-toluenesulfonate (CMC) in 100 mM pH 7.0 potassium phosphate buffer in H_2O (20 mg CMC/10 mL buffer) followed by 30-40 μM cytochrome *c* solution in 4.4 mM pH=8 potassium phosphate buffer.

Voltammetry was used to quantify the surface coverage after the covalent assemblies were rinsed with different solutions. First, the assemblies were rinsed with 4.4 mM phosphate buffer (I≈10 mM, pH=8), after which cyclic voltammograms were collected in 40 mM phosphate buffer (I=80 mM, pH=7, the same buffer used for voltammetry in this study). The electrodes were then removed from the buffer solution and rinsed with 100 mM phosphate buffer (I=200 mM, pH=7) and voltammograms were once again collected at the same scan rates in the I=80 mM buffer. The procedure was repeated a final time using 1 M KCl as the rinse solution.

Because of the difficulty in obtaining reliable voltammetry at low scan rates, voltammograms were taken at 10 V/s. Since the rate constants for $(CH_2)_5COOH/(CH_2)_4OH$ assemblies were determined using CVs taken from 10 V/s – 1000 V/s, this procedure was

deemed acceptable (see II). The cytochrome *c* surface coverage was determined both in pmol/cm^2 and as a percentage ratio of largest recorded surface coverage for a given electrode. The formal potential, peak separation, and FWHM were also recorded. These quantities are reported in Tables 1 and 2.

Table 1. Surface coverage and percentage surface coverage for electrostatic and covalent assemblies rinsed with progressively higher ionic strength solutions.

	Surface coverage (pmol/cm^2)	
Rinse solution (ionic strength)	**Electrostatic Assemblies**	**Covalent Assemblies**
10 mM phosphate buffer	1.12 ± 0.62	1.72 ± 0.78
200 mM phosphate buffer	0.55 ± 0.45	0.81 ± 0.59
1 M KCl	0.36 ± 0.45	0.77 ± 0.54

Table 2. Voltammetric properties for electrostatic and covalent assemblies rinsed with progressively higher ionic strength solutions.

	$E^{0'}$ (mV)	$E^{0'}$ (mV)
Rinse solution (ionic strength)	**Electrostatic Assemblies**	**Covalent Assemblies**
10 mM phosphate buffer	-12 ± 9	-13 ± 8
200 mM phosphate buffer	-17 ± 14	-18 ± 5
1 M KCl	10 ± 8	-15 ± 6
	ΔE_p (mV)	**ΔE_p (mV)**
Rinse solution (ionic strength)	**Electrostatic Assemblies**	**Covalent Assemblies**
10 mM phosphate buffer	23 ± 12	24 ± 12
200 mM phosphate buffer	45 ± 35	30 ± 21
1 M KCl	109 ± 41	25 ± 21
	FWHM (mV)	**FWHM (mV)**
Rinse solution (ionic strength)	**Electrostatic Assemblies**	**Covalent Assemblies**
10 mM phosphate buffer	124 ± 7	118 ± 9
200 mM phosphate buffer	142 ± 23	123 ± 10
1 M KCl	150 ± 15	127 ± 12

t-tests were performed at a 95% confidence level, and the following values were found to be significantly different: $E^{0'}$(covalent) and $E^{0'}$(electrostatic) rinsed with 1 M KCl, ΔE_p(covalent) and ΔE_p(electrostatic) rinsed with 1 M KCl and FWHM(covalent) and FWHM(electrostatic) for 1 M KCl. This seems to indicate that there is little or no difference between $E^{0'}$ and reversibility (at 10 V/s) of covalent and electrostatic assemblies rinsed with I = 10 mM or I = 200 mM

phosphate buffer at 10 V/s. However, these properties differ significantly following rinsing with 1 M KCl, even though the surface coverage does not significantly change.

II. Rinsing study of covalent assemblies with rate monitoring

Electrodes were prepared as in Section I. Assemblies were rinsed five times with I = 10 mM pH = 8 potassium phosphate buffer, and CVs were taken at 10, 20, 50, 100, 200, 500 and 1000 V/s. The assemblies were then rinsed five times with I = 200 mM, pH = 7 phosphate buffer and the same voltammograms collected. Trumpet plots were constructed for each voltammogram set and rate constants assigned by fitting the points to a Marcus theory curve.

The surface coverage, $E^{0'}$ and rate constants are reported for both types of assemblies in Table 3. The voltammetric peaks for electrostatic assemblies rinsed with I = 200 mM phosphate buffer did not form a consistent curve, and so the rate constant reported in Table 3 is a fit to the peak separation at 10 V/s.

Table 3. Surface coverages, rate constants, and formal potentials for electrostatic and covalent assemblies rinsed sequentially with low and high ionic strength buffer.

	I=10 mM rinse		I=200 mM rinse	
	electrostatic	**covalent**	**electrostatic**	**covalent**
Coverage‡ (pmol/cm^2)	0.92 ± 0.54	1.15 ± 0.30	0.29 ± 0.19	0.59 ± 0.11
k^0 (s^{-1})	4300 ± 270	4800 ± 650	360 ± 410†	5800 ± 1000
$E^{0'}$ (mV)	-11 ±10	-14 ±2	-16 ± 14	-18 ± 3

‡measured at 10 V/s.
†the voltammetric peaks did not form a consistent curve for these scan rates; the peak separation at the 10 V/s scan rate gives the value reported here.

At 95% confidence, *t*-tests demonstrate that the surface coverage and k^0 of electrostatic and covalent assemblies is not significantly different after rinsing with I = 10 mM phosphate buffer. Following rinsing with I = 200 mM phosphate buffer, the surface coverage for electrostatic assemblies is not significantly different from covalent assemblies; however the k^0

values are significantly different from one another. This fact is reflected by the drastic change in the quality of the trumpet plots for electrostatic assemblies with I = 200 mM rinsing; see Figure 1.

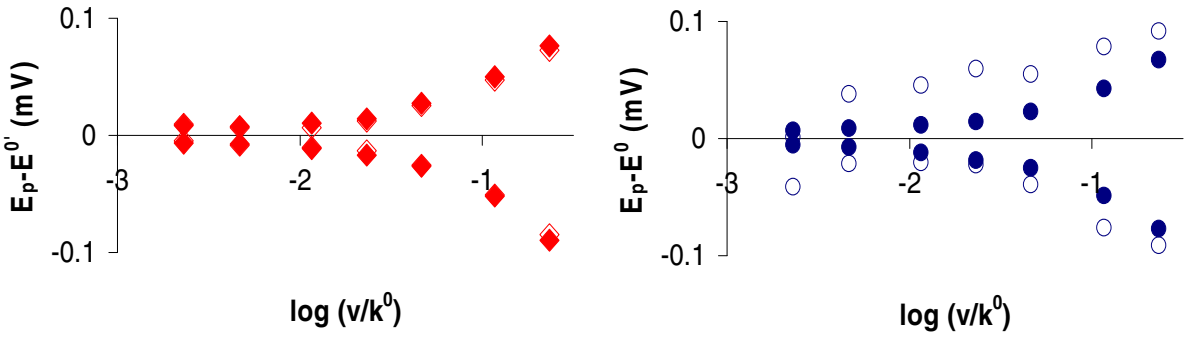

Figure 1. Trumpet plots for covalent (red diamonds) and electrostatic (blue circles) assemblies following rinsing with I = 10 mM phosphate buffer (closed symbols) and I = 200 mM phosphate buffer (open symbols). Voltammograms were taken at 0.1, 1, 10, 20, 50, 100, 200, 500 and 1000 V/s.

Figure 2 shows simulated voltammograms which contain contributions from a fast population (k^0 = 5783 s^{-1}; $E^{0'}$ = -18 mV) and a slow electrostatic population (k^0 = 360 s^{-1}; $E^{0'}$ = -16 mV or 1346 s^{-1}; $E^{0'}$ = -5 mV). These values were chosen to reflect k^0 and $E^{0'}$ as measured for covalent (fast) and electrostatic (slow) assemblies that had been rinsed with I = 200 mM buffer (see Table 3). The ratio between the two populations was allowed to vary, and the shape of the resulting voltammograms can be seen in Figure 2.

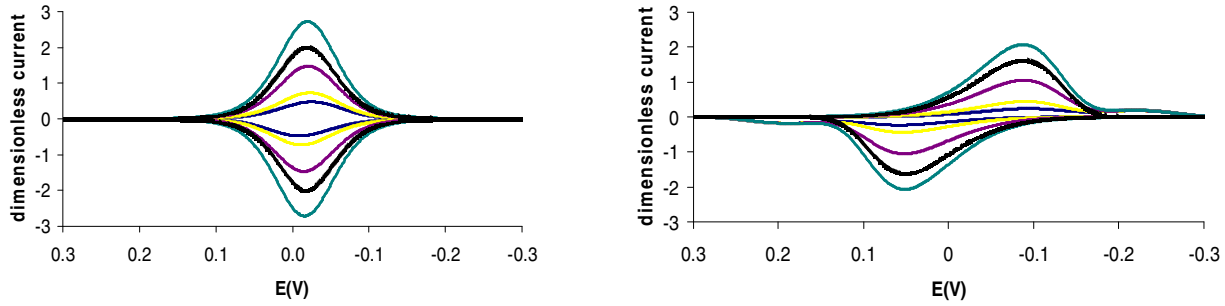

Figure 2. Simulated cyclic voltammograms for covalently attached and electrostatically adsorbed cytochrome *c* present in differing amounts on the same electrode following rinsing with I = 200 mM phosophate buffer. Voltammograms were simulated at 10 V/s (left) and 1000 V/s for a covalent population with a rate constant of 5800 s^{-1} and $E^{0'}$=-18 mV and an electrostatic population having k^0=360 and $E^{0'}$=-16. From inward to outward, voltammograms correspond to the following ratios (covalent: electrostatic): 1:1 (blue), 2:1 (yellow), 5:1 (purple), no electrostatic present (black textured, scaled by a factor of 8 for better visibility) and 10:1 (teal).

A second, slower population, as long as it is present in a lesser amount than the faster population, does not strongly affect the peak position. This finding is evident from Table 4, which compares the E(cathode) for a simulated purely covalent population (k^0=5783 s^{-1}; see Table 3) to those casess where a slower population was also present. At higher proportions of slow population (1:1 in Table 4) the shift in peak position induced by the slow population becomes more pronounced, and it causes the peak separation to be larger for situations where a large enough amount of the slow population is present. We find an opposite trend in our covalent assemblies of cytochrome *c*; i.e. the peak separation decreases with rinsing by I = 200 mM buffer rather than increasing. This decrease reflects a decrease in the population of the slow, electrostatic species, and the higher rate of the covalently bound protein.

Table 4. Simulated E(cathode) values for a "covalent" population mixed with a slower population.

Scan rate (V/s), slow k^0 (s^{-1})	covalent:electrostatic (molar ratio)				
	1:0*	**1:1**	**2:1**	**5:1**	**10:1**
10 V/s, k^0(slow) = 360 s^{-1}	-18 mV	-26 mV	-23 mV	-21 mV	-20 mV
1000 V/s, k^0(slow) = 360 s^{-1}	-87 mV	-94 mV	-90 mV	-88 mV	-87 mV

*no slow population present; analogous to a purely covalent population.

From these results, electrostatic and covalent assemblies respond very differently to high ionic strength rinsing, so that the electrostatic assemblies are a factor of two or more lower in coverage. This fact, coupled with a much slower electron transfer for the electrostatic assemblies treated in this way leads to a voltammetric response that is dominated by the covalently attached cytochrome *c*. The origin of the slowing of the rate constant in the electrostatic assemblies remains under investigation.

III. Determining the tunneling decay coefficient

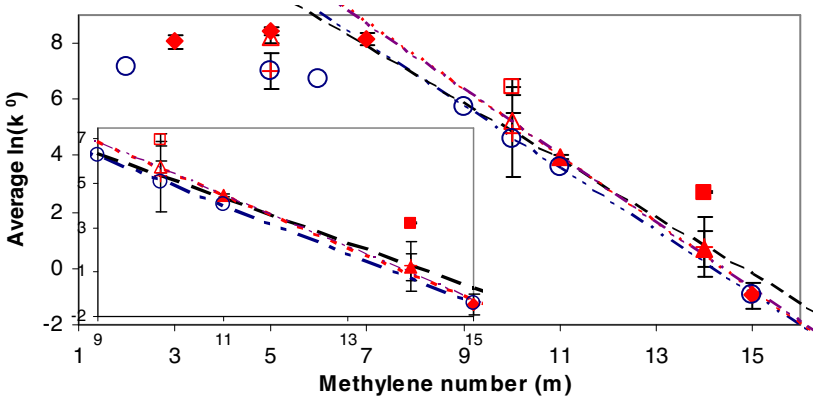

The rate constant is fit to an exponential decay, which is expected for a tunneling mechanism. The dashed blue line corresponds to the tunneling rate constant in electrostatic systems, the black line to covalent systems on pure –COOH-terminated SAMs, the red line to C_mCOOH/C_mOH or $C_{m\pm1}OH$, and the purple line to combined pure and mixed films. Inset: magnification of the tunneling region.

IV. Calculating $\frac{V_{rms,c}}{V_{rms,e}}$

$$\frac{\left|V_{rms,c}\right|^2}{\left|V_{rms,e}\right|^2} \propto \frac{k_C^0}{k_E^0} = \frac{k_C^0(x=0)\exp(-\beta_C m)}{k_E^0(x=0)\exp(-\beta_C m)}$$

$$= \frac{\exp(16.91 \pm 0.99)\exp[(-1.15 \pm 0.2)m]}{\exp(15.75)\exp(-1.10m)}$$

$$= (3.16 \pm 0.18)\exp[(-0.07 \pm 0.058m)]$$

Supplying values for m that lie in the tunneling region yields the following ratios for $\frac{\left|V_{rms,c}\right|^2}{\left|V_{rms,e}\right|^2}$ and $\frac{\left|V_{rms,c}\right|}{\left|V_{rms,e}\right|}$:

m	$\frac{\left\|V_{rms,c}\right\|^2}{\left\|V_{rms,e}\right\|^2}$	$\frac{\left\|V_{rms,c}\right\|}{\left\|V_{rms,e}\right\|}$
8	3.2 ± 0.5	1.8 ± 0.1
11	1.5 ± 0.4	1.2 ± 0.2
13	1.3 ± 0.7	1.1 ± 0.3
15	1.1 ± 0.8	1.1 ± 0.4